Variables Affecting the Testing of Pavements by the Surface Waves Method

DENNIS R. HILTUNEN AND RICHARD D. WOODS

The spectral analysis of surface waves (SASW) method is a nondestructive testing procedure under development for determining the elastic modulus profile of pavement systems in situ. The ultimate objective for practical use of the SASW method is the design of a totally automated, movable test rig for investigating pavement systems. An important step toward this objective would be the development of a multiple-transducer testing procedure in which the source-to-near-receiver distance S and source type are significant variables. Tests conducted on two asphaltic concrete pavements to study the effects of these variables determined that the ratio of S to receiver spacing X should be ≤ 2. In addition, dispersion data were independent of S when wavelengths longer than $2X$ were eliminated from the data. The effect of source type on the ranges of useful frequencies for a given value of X was significant. In general, both the lower and upper cutoff frequencies decreased as the weight of the source increased. The dispersion curves generated with the data were compared with optimum ones using a constant source type. Although no single source type consistently yielded an optimum dispersion curve, combining the data from a 4-oz ball peen hammer and an 8-lb sledge hammer yielded an optimum dispersion curve over all wavelengths.

In pavement engineering, in situ values of elastic moduli are important parameters in the determination of overlay thicknesses and allowable loads for existing pavement structures and for assessment of other rehabilitation needs. Elastic moduli for pavement systems are typically determined in situ by deflection-based measuring devices such as the falling weight deflectometer (FWD). Modulus values are determined from the deflection measurements through use of multilayer elastic analysis. Deflection techniques, however, have well-known limitations. First, the backcalculation of moduli from deflection measurements for pavements with thin surface layers is nearly impossible because of the insensitivity of the deflection basin to the stiffness of the thin surface layer (*1,2*). Second, the deflection procedures must assume values for the thicknesses of the pavement layers or determine the values from cores (*1,3*). Third, the deflection procedures are only capable of determining an average modulus to represent each pavement layer, when in fact the modulus usually varies throughout the layer (*4*). Fourth, the deflection procedures use a static model of the pavement system to backcalculate the moduli, despite the dynamic nature of the test itself (*5–9*). It is seen, therefore, that an improved nondestructive method of determining in situ stiffness profiles of pavement systems is needed.

D. R. Hiltunen, Department of Civil Engineering, Pennsylvania State University, University Park, Pa. 16802. R. D. Woods, Department of Civil Engineering, University of Michigan, Ann Arbor, Mich. 48109.

A new method for measuring in situ elastic modulus profiles, the spectral analysis of surface waves (SASW), has been under continuous development since 1980. The SASW method is based on the generation and detection of Rayleigh waves from the surface of the pavement system. Although the main disadvantage of SASW is that the testing and data reduction are slow, it is felt that with continued research and development the testing and data reduction time can be substantially reduced. Previous work conducted at the University of Michigan to further the development of the SASW method has also been reported (*10*).

THE SASW METHOD

The SASW method is a testing procedure for determining elastic modulus profiles of pavement systems in situ. The test is performed on the pavement surface. Measurements are made at strain levels below 0.001 percent, where elastic properties of pavement materials are considered independent of strain amplitude. The key elements in SASW testing are the generation and measurement of Rayleigh waves.

Several publications (*10–18*) in recent years have described the SASW method in detail. A schematic of the experimental arrangement for SASW tests is shown in Figure 1. Current practice calls for locating two vertical receivers on the pavement surface a known distance apart. Then a transient wave containing a large range of frequencies is generated in the pavement by means of a hammer. The surface waves are detected by the receivers and recorded using a Fourier spectrum analyzer. The analyzer is used to transform the waveforms from the time domain to the frequency domain and then to perform spectral analyses on them. The spectral analysis functions of interest here are the phase information of the cross power spectrum and the coherence function. Knowing the distance and the relative phase shift between the receivers for each frequency, the phase velocity and wavelength associated with that frequency are calculated. The final step is application of an inversion process that constructs the elastic modulus profile from the phase velocity versus wavelength (dispersion curve) information.

The principal advantage of using the SASW method for pavement evaluation is its capabilities for determining

- The elastic modulus of thin pavement surface layers (*15,19*);
- The thicknesses of pavement layers (*13,15,17–19*);
- The variation of elastic modulus within a given pavement layer, i.e., values of the modulus gradient (*13,15–16*); and
- The elastic moduli of the pavement system in the presence of bedrock close to the surface (*15*).

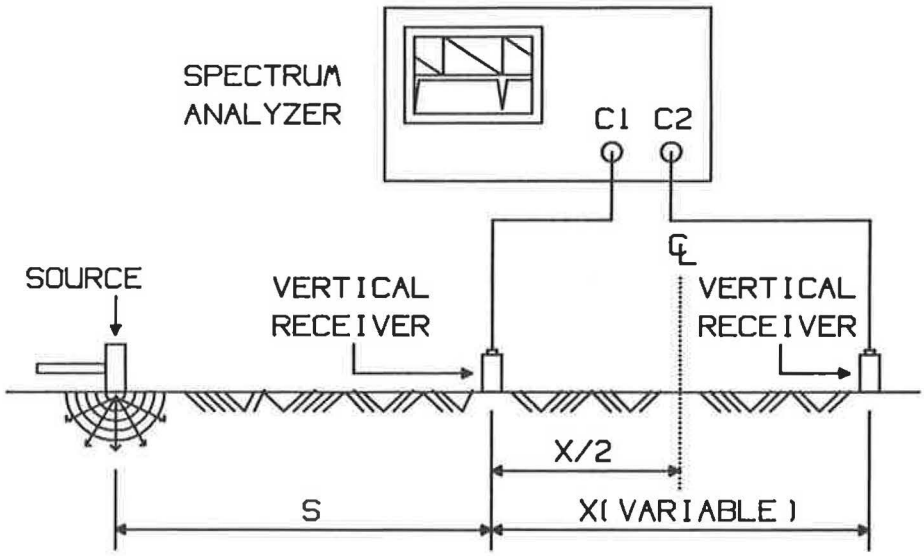

FIGURE 1 Schematic of experimental arrangement for SASW tests [after Nazarian (*12*)].

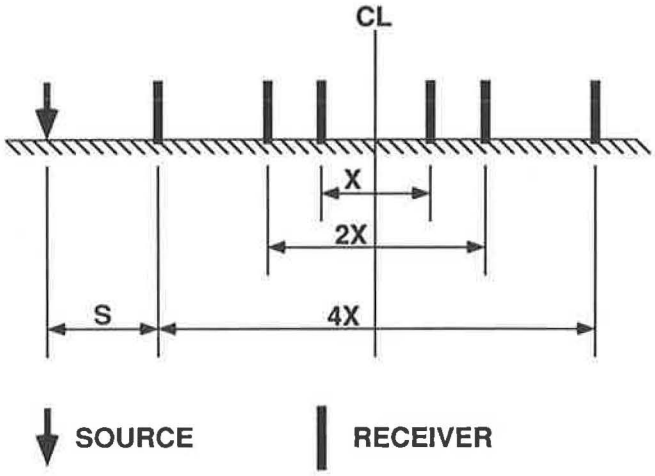

FIGURE 2 Multiple transducer configuration using six transducers and CRMP geometry.

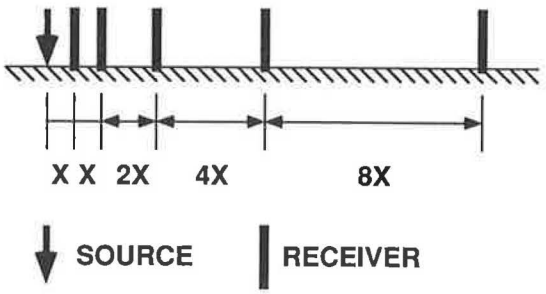

FIGURE 3 Multiple transducer configuration using five transducers and CS geometry.

These capabilities would provide a useful supplement to the deflection-based procedures, specially for cases in which the deflection procedures suffer from the limitations detailed earlier.

The ultimate objective for the SASW method is a totally automated, self-contained, movable test rig for investigating pavement systems. An important step toward this objective is the development of a multiple-transducer testing procedure in which all the data for a given site can be obtained with the least number of source excitations on the test surface as possible. Currently, the SASW method is conducted using only two transducers, primarily because a two-channel spectrum analyzer is a convenient means of collecting and observing the data in the field. This means of data collection requires a good deal of time, because several different receiver spacings are usually required to fully investigate a site. The extension of this procedure to more than two transducers, i.e., to a multiple-transducer testing procedure, thus seems appropriate.

Hiltunen and Woods (*20*) suggested two possible multiple-transducer arrays, one on the basis of the common receivers' midpoint (CRMP) geometry (Figure 2), and the other on the common source (CS) geometry (Figure 3). They further suggested that to implement a multiple-transducer array, the following characteristics of the two-transducer array relative to receiver separation X and source-receiver distance S must be determined:

- The source-receiver scaling geometry most appropriate for testing pavements (by varying X while keeping $S = X$ and varying the position of the receivers' midpoint relative to the source); and
- The best source location (by varying S, while keeping X constant).

Furthermore, the most appropriate source type should be determined.

Hiltunen and Woods (*20*) have presented results from tests conducted at an asphaltic concrete pavement site that suggest that SASW measurements are independent of source-receiver scaling geometry. In the present work, tests were conducted to investigate the effects of S and source type on the measurements. Results from the entire test program are summarized

and a multiple-transducer configuration for pavement testing is suggested.

PREVIOUS RESEARCH

Source-to-Near-Receiver Distance (S)

Nazarian (*12*) has discussed the factors that limit the range of possible values of S. The source should be far enough away from the near receiver that a significant amount of the body wave energy dies out before arriving at the near receiver. However, if the source is too far away from the receivers, the Rayleigh wave energy associated with the frequencies of interest may not be sufficient for detection by the receivers, and background noise may dominate the record.

On the basis of experimental studies, Heisey et al. (*11*) have suggested that $S = X$ is adequate, provided that wavelengths $< 0.5X$ or $> 3X$ are eliminated from the data.

However, theoretical studies conducted by Sanchez-Salinero et al. (*21*) have indicated criteria that are drastically different from the experimental results of Heisey et al. (*11*). For CRMP geometry with $S = X$, and assuming plane Rayleigh waves [as the inversion program INVERT (*12*) does], they suggest that the field data be filtered for wavelengths $> 0.5X$.

The disparity between experimental and theoretical results is evident in this discussion. More important, however, it is evident that little work has been done to systematically study the effects of S by changing its value over a range. Yet, the results of such a study would be vital to the development of a multiple-transducer array using a fixed source location. Therefore, tests were conducted to examine this question.

Source Type

Nearly all previous work on the SASW method has somehow addressed the issue of source selection, particularly sources for impact testing. It has been clearly demonstrated that the choice of source depends on the frequency range of interest. Small, lightweight sources produce high frequencies necessary for sampling shallow depths, while larger, heavier sources produce low frequencies for sampling greater depths. The intent here was not to reaffirm these findings. Rather, the questions that arise when confronted with implementing a multiple-transducer array is how many sources are required and of what size.

Past work has shown that when conducting SASW tests using two receivers it is often necessary to use a different source for each receiver spacing. However, this process often results in overlap in the dispersion curve data for different receiver spacings. This overlap provides some insurance that the data obtained are reliable, but it may be possible to adequately sample a site with fewer sources if some of the overlap in data for different receiver spacings is redundant. Thus, two series of tests were conducted to determine the minimum number of sources necessary for adequately defining the dispersion curve for a site. The sources under investigation were all of the impact type and conclusions obtained were valid for this type of excitation.

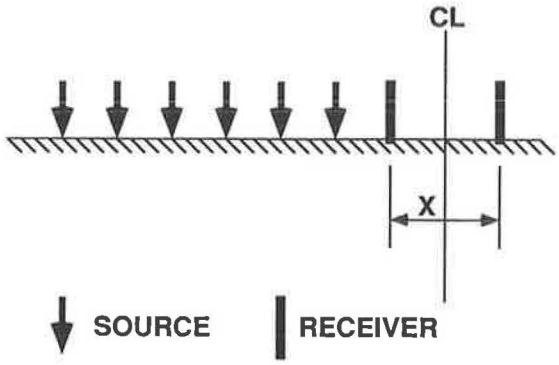

FIGURE 4 Schematic of two-transducer tests using CRMP geometry and various source-to-near-receiver distances.

DISCUSSION OF TESTS

Sites and Geometries Selected

The tests to study the effects of S and source type were conducted at two asphaltic concrete pavement sites. The first series of tests was conducted at the G. G. Brown parking lot site on the University of Michigan campus in August 1986. The second series of tests was conducted at the SEMTA parking lot site in Livonia, Michigan, in June 1987.

A schematic of the two-transducer tests conducted to examine the effects of S is shown in Figure 4. The transducer placement followed the CRMP geometry in that each transducer pair was placed symmetrically about the same imaginary centerline. Transducer spacings of 0.5, 1, 2, 4, and 8 ft were examined. The range of source locations used at each receiver spacing X limited values of the ratio S/X to the range 0.5 to 3. The intent was to determine the optimum value for S/X and to provide guidance in developing the geometry for a multiple-transducer array.

The effects of source type were studied both at the G. G. Brown and SEMTA parking lot sites. During the CS geometry tests at the SEMTA parking lot site (*20*), data were collected using five source types at each receiver spacing. The sources ranged in weight from 4 oz (a ball peen hammer) to 8 lb (a sledge hammer). The effects of source and receiver geometry have been studied by Hiltunen and Woods (*20*) using the optimum source (see Table 1) for each receiver spacing; data for other sources are examined herein. Table 1 presents such data obtained from the tests at the SEMTA parking lot site.

Useful Frequency Ranges

Tables 2–4 present useful frequency ranges from cross power spectrum and coherence function data as functions of S and source type. The cross power spectrum and coherence function data collected in the field have also been used to determine Rayleigh wave dispersion curves (*10,12*). Part of this process requires determining frequency ranges in which useful data exist. Because S and source type affect the ranges of useful frequencies, they ultimately determine how well the dispersion curves are defined. For a given test setup, as more frequencies are eliminated because of poor phase or poor coherence, the less well defined the dispersion curves become.

TABLE 1 TEST PARAMETERS FOR SEMTA PARKING LOT SITE

Receiver Spacing (ft)	Receiver Type	Frequency Span (Hz)	Source Type[a]
0.5	Accel.	10000	4 oz[b]
0.5	Accel.	10000	8 oz
0.5	Accel.	10000	16 oz
0.5	Accel.	10000	40 oz
0.5	Accel.	10000	128 oz
1	Accel.	6250	4 oz[b]
1	Accel.	6250	8 oz
1	Accel.	6250	16 oz
1	Accel.	6250	40 oz
1	Accel.	6250	128 oz
2	Velocity	1000	4 oz
2	Velocity	1000	8 oz
2	Velocity	1000	16 oz[b]
2	Velocity	1000	40 oz
2	Velocity	1000	128 oz
4	Velocity	800	4 oz
4	Velocity	800	8 oz
4	Velocity	800	16 oz
4	Velocity	800	40 oz[b]
4	Velocity	800	128 oz
8	Velocity	250	4 oz
8	Velocity	250	8 oz
8	Velocity	250	16 oz
8	Velocity	250	40 oz
8	Velocity	250	128 oz[b]

[a] Refers to the weight or size rating of hand-held hammer used as impact source.

[b] "Optimum" source for given receiver spacing.

TABLE 2 USEFUL FREQUENCY RANGES FOR 0.5-ft RECEIVER SPACING X AS A FUNCTION OF SOURCE-TO-NEAR-RECEIVER DISTANCE S AT SEMTA PARKING LOT SITE

Source-to-Near-Receiver Distance (S) (ft)	S/X	Lower Cutoff Frequency (Hz)	Upper Cutoff Frequency (Hz)
0.25	0.5	112	5800
0.50	1.0	125	5875
0.75	1.5	887	5900
1.00	2.0	1000	5950
1.25	2.5	1000	5000
1.50	3.0	1050	4100

TABLE 3 USEFUL FREQUENCY RANGES FOR 0.5-ft RECEIVER SPACING X AS A FUNCTION OF SOURCE-TO-NEAR-RECEIVER DISTANCE S AT G. G. BROWN PARKING LOT SITE

Source-to-Near-Receiver Distance (S) (ft)	S/X	Lower Cutoff Frequency (Hz)	Upper Cutoff Frequency (Hz)
0.25	0.5	100	8900
0.50	1.0	125	9250
0.75	1.5	100	8125
1.00	2.0	100	6650
1.50	3.0	125	2800

Tables 2–4 of the useful frequency ranges determined from each cross power spectrum and coherence function pair were developed as a representative example because of the large amount of data collected. The minimum- and maximum-frequency cutoffs for each pair were determined as functions of S and source type. The effects of S and source type were significant.

Source-to-Near-Receiver Distance

Ranges of useful frequencies as functions of S for the 0.5-ft receiver spacing at the SEMTA parking lot site are presented in Table 2; similar data for the G. G. Brown parking lot site are presented in Table 3. Results for the remaining receiver spacings have been provided by Hiltunen (*10*).

The upper cutoff frequency decreases significantly for $S/X > 2$. This decrease in the upper cutoff frequency is specially important for the testing of pavements because high frequencies are required to define the dispersion curve of the shallow portions of the pavement system. Inadequate definition of the high-frequency portion of the dispersion curve would result in an inaccurate modulus profile for all layers in the system. Thus, S/X should be ≤ 2 for SASW testing of pavements. The complete sets of data from both test sites strongly support this conclusion (*10*).

TABLE 4 USEFUL FREQUENCY RANGES FOR 0.5-ft RECEIVER SPACING X AS A FUNCTION OF SOURCE TYPE AT SEMTA PARKING LOT SITE

Source Type	Lower Cutoff Frequency (Hz)	Upper Cutoff Frequency (Hz)
4 oz	100	6375
8 oz	100	6012
16 oz	87	5950
40 oz	75	5300
128 oz	62	5250

Source Type

The ranges of useful frequencies as a function of source type for the 0.5-ft receiver spacing at the SEMTA parking lot site are shown in Table 4. The results for the remaining receiver spacings and for the G. G. Brown parking lot site have been provided by Hiltunen (*10*).

The weight of the source had a dramatic influence on the dispersion curves obtained. In general, both the upper and lower cutoff frequencies decreased as the weight of the source increased. The complete sets of data (*10*) from both test sites strongly support these observations.

Magnitude of the Cross Power Spectrum

The magnitude of the cross power spectrum is defined to be the product of the magnitudes of the two signals. As a measure of the mutual power between two sources, it is thus useful for isolating signals that are common to both. For SASW testing, the cross power spectrum establishes the energy distribution as a function of frequency common to both signals. When the energy is high compared to the background noise, good coherence and thus good data are expected. Conversely, when the energy is low compared with background noise, poor coherence and thus bad data are expected. The magnitude of the cross power spectrum is thus useful for explaining the effects of S and source type on the dispersion curves.

Source-to-Near-Receiver Distance (S)

Examples of magnitudes of the cross power spectra as a function of S for the 0.5-ft receiver spacing at the SEMTA parking lot site are shown in Figures 5 and 6. [Additional plots for the SEMTA and G. G. Brown parking lot sites have been provided by Hiltunen (*10*).] Each plot contains the spectra for S/X = 0.5, 1.0, 1.5, 2.0, 2.5, and 3.0, for the given receiver

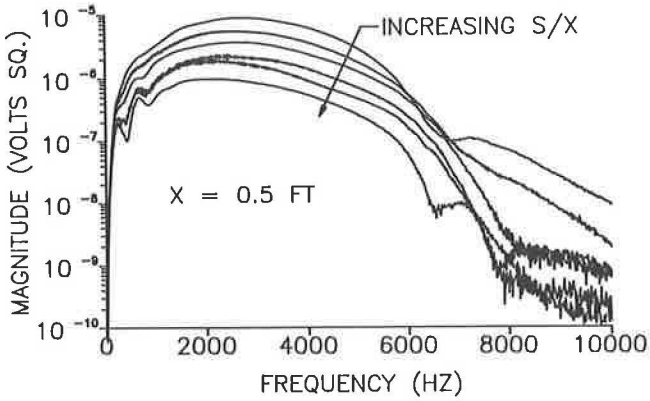

FIGURE 5 Magnitude (absolute) of cross power spectrum as a function of source-to-near-receiver distance S for X = 0.5 ft at SEMTA parking lot site.

spacing. The spectra on each plot are difficult to separate, but it is not necessary that they be individually distinguished. The trend is more important. Therefore, each spectrum is presented in two formats. First (Figure 5), the actual or absolute magnitudes are shown as recorded in the field. The second plot (Figure 6) shows relative magnitudes, defined as the absolute magnitude divided by the peak magnitude for each spectrum. The plot of absolute magnitudes indicates how the actual energy levels change with S for the given value of X. The plot of relative magnitudes indicates how the shape of the energy distribution over frequency varies with S for the given value of X.

The absolute magnitude of the cross power spectrum decreases with increasing S/X, partially because of geometric damping of the signals. This fact alone does not account for the decrease in upper cutoff frequency as S/X increases. For a perfectly elastic system, the shape of the cross power spectrum should be independent of S, because the only damping present in the system is geometric, and therefore does not

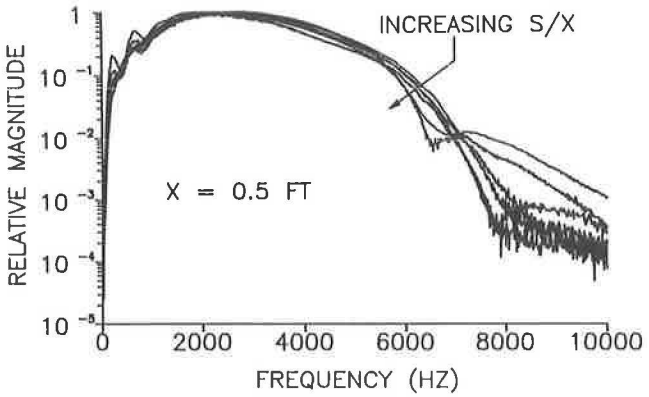

FIGURE 6 Magnitude (relative) of cross power spectrum as a function of source-to-near-receiver distance S for X = 0.5 ft at SEMTA parking lot site.

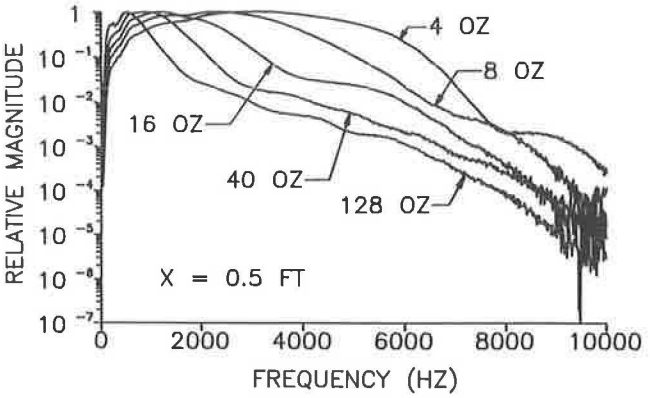

FIGURE 8 Magnitude (relative) of cross power spectrum as a function of source type for X = 0.5 ft at SEMTA parking lot site.

depend on the frequency of the waveform. However, in a real system, e.g., pavement, material damping of the waveform will occur as well. Material damping is frequency dependent. Higher frequency waves attenuate more than lower frequency waves over the same propagation distances in the same pavement because they undergo more cycles of motion. The plots, e.g., in Figure 6, of relative magnitude of the cross power spectrum show this point quite clearly. For the given receiver spacing, the spectra as a function of S/X do not coincide as they would if the system under test was perfectly elastic. In addition, the magnitudes of the high-frequency components dramatically decrease and the upper cutoff frequencies also decrease as S/X increases because of the material damping. For $S/X > 2$, the high-frequency components of the waveforms attenuate excessively and become buried in background noise. Poor phase data and poor coherence data result. [The complete data set (*10*) strongly supports these observations.]

Source Type

Examples of the magnitudes of the cross power spectra as functions of source type for the 0.5-ft receiver spacing at the SEMTA parking lot site are shown in Figures 7 and 8. Each plot contains the spectra for each source type studied at the given receiver spacing. Further, each spectrum is presented in absolute and relative formats. [Again, additional spectra for the SEMTA and G. G. Brown parking lot sites have been provided by Hiltunen (*10*).]

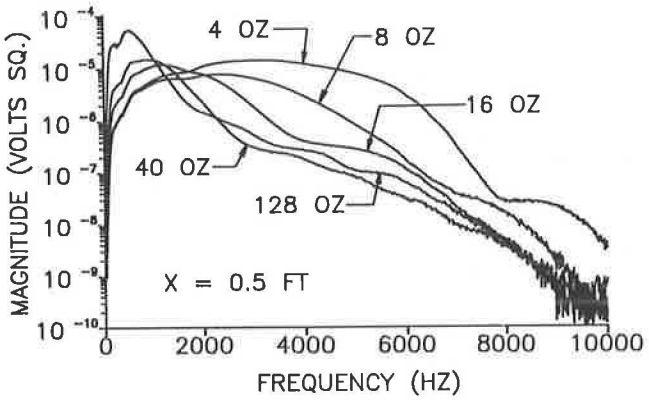

FIGURE 7 Magnitude (absolute) of cross power spectrum as a function of source type for X = 0.5 ft at SEMTA parking lot site.

The effect of source type on the magnitude of the cross power spectrum is similar to that of S. However, the underlying reasons for the observed trends are different. Although material damping explains the effect of S, the mechanics of the source impulse explains the effect of source type.

The time signal of the force created by each hammer is an impulse, i.e., the duration of the force is very small in comparison to the total record length. The energy distribution of an impulse signal in the frequency domain is inversely proportional to the time duration of the impulse. In a short-duration impulse, the energy is spread over a wide frequency band, whereas in a longer duration impulse the energy is concentrated at low frequencies. The impulse duration for a specific source is determined by the elasticity of the materials of the structure and source that are in contact during impact and on the mass of the source. In the present case, the structure (pavement) is the same for all sources. In addition, all of the sources used are steel hammers. Thus, the only remaining factor is the weight of the source. The duration of the impulse is directly proportional to the weight of the source. Thus, light hammers produce a short impulse and distribute the energy over a wide frequency band, whereas heavier hammers produce a longer impulse and concentrate the energy at lower frequencies. Exactly this behavior is observed in the plots of the cross power spectrum magnitudes. In the low-frequency range of the absolute magnitude plots, the energy levels are largest for the heavier hammers. However, the relative magnitude plots reveal that the light hammers distribute the energy over a much wider frequency band.

The cutoff frequencies are the result of poor phase or poor coherence data. The poor data occur at frequencies at which the signals contain a large proportion of background noise. Thus, the lower cutoff frequency decreases with increasing hammer weight because the heavier hammers concentrate more energy at low frequencies. The upper cutoff frequency increases with decreasing hammer weight because the lighter hammers concentrate energy at higher frequencies while distributing the energy over a wider frequency band. [Again, the complete data set (*10*) strongly supports these observations.]

Combined Dispersion Curves for Constant X/L_R, Where L_R Is the Rayleigh Wavelength

The effect of S on the range of useful data collected in the field has been discussed. S also affects the resulting dispersion curve and thus the interpreted stiffness profile.

A criterion for filtering data for wavelengths that are inappropriate for the spacing of the receivers has been given for a test setup for which $S/X = 1$ (*11*). According to this criterion, wavelengths smaller than one-half the receiver spacing and greater than three times the receiver spacing are eliminated. In other words, for a given receiver spacing, waves that have traveled for less than one-third cycle or greater than two cycles are filtered out.

Sanchez-Salinero et al. (*21*) studied the wavelength-receiver spacing filter criterion from a theoretical point of view. In the SASW method, it is assumed that because about two-thirds of the energy generated by the source is transmitted by Rayleigh waves, and because these waves attenuate less than body waves, the wavetrain passing by the receivers is composed primarily of Rayleigh waves. It is further assumed that the Rayleigh waves are plane waves, i.e., generated by a source at infinity.

These assumptions lead to the question of the number of cycles the wave must travel before these assumptions are valid. To examine this question, a series of analytical studies that simulate the testing procedure was performed. Theoretical dispersion curves were generated by two methods, one that assumes plane Rayleigh waves only, and one that includes the Rayleigh and body waves generated by a point source located at a finite distance from the receivers. The studies were performed for test setups such that $S/X = 1$. Further, dispersion curves generated by the method that included the body waves were for constant values of X/L_R, the ratio of the receiver spacing to the wavelength of the Rayleigh wave. In other words, the curves were generated for constant values of the number of cycles the waves traveled. By comparing the dispersion curves for different values of the X/L_R ratio with the curve generated by assuming only plane Rayleigh waves, the number of cycles necessary for the wave to travel before the assumption is valid was established. Sanchez-Salinero et al. (*21*) found that for a test setup in which $S = X$, the field data should be filtered for wavelengths $> 0.5X$. Thus, the assumption that only plane Rayleigh waves exist is best when the wave has traveled two or more cycles.

The disparity between the experimental and theoretical criterion should be observed. Heisey et al. (*11*) suggest that waves traveling more than two cycles will attenuate excessively and thus should be eliminated from the collected data, whereas Sanchez-Salinero et al. (*21*) suggest that the waves must travel at least two cycles to prevent contamination by body waves. Which criterion should be used for analyzing field data from SASW tests? If the entire wavetrain attenuates excessively after two cycles, as the experimental results indicate, after how many cycles do the body waves attenuate to an insignificant level? Some insight into these questions can be gained by examining the data collected as part of this research. If the experimental dispersion curves for constant values of X/L_R are compared as a function of S/X, some indication of the body wave attenuation can be obtained. For a given value of X/L_R, as the source is moved further from the receivers, the wavetrain at the receivers should contain a higher percentage of Rayleigh wave energy. When the body wave energy attenuates to an insignificant level, i.e., the value of X/L_R becomes large enough, the dispersion curves for all values of S/X should be the same because the only energy of significance is from the Rayleigh wave.

Many experimental dispersion curves for constant values of X/L_R as a function of S/X for the G. G. Brown and SEMTA parking lot sites have been provided by Hiltunen (*10*). Two examples of dispersion curves for values of X/L_R between 0.2 and 2 are shown in Figures 9 and 10.

The measured phase velocities are practically independent of S/X for wavelengths > 5 ft for all values of X/L_R. (The data for all values of S/X are nearly the same.) This condition suggests that wavelengths larger than approximately 5 ft are not contaminated with body wave energy. Thus, body wave energy is only significant in the upper layers of the pavement system.

Second, the measured phase velocities are significantly dependent on S/X for small values of X/L_R for wavelengths < 5 ft (Figure 9). In particular, the measured phase velocities generally increase with decreasing S/X for a given value of X/L_R. This relation suggests that body wave energy is present in the signals. The velocities both of compression and shear waves exceed that of the Rayleigh wave. As the source is moved closer to the first receiver, the amount of body wave energy in the signals increases. The expected increase in measured velocity is exactly what has been measured.

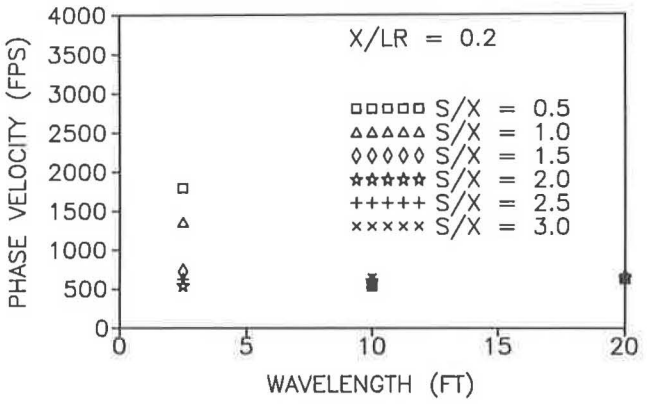

FIGURE 9 Experimental dispersion curves for $X/L_R = 0.2$ at G. G. Brown parking lot site.

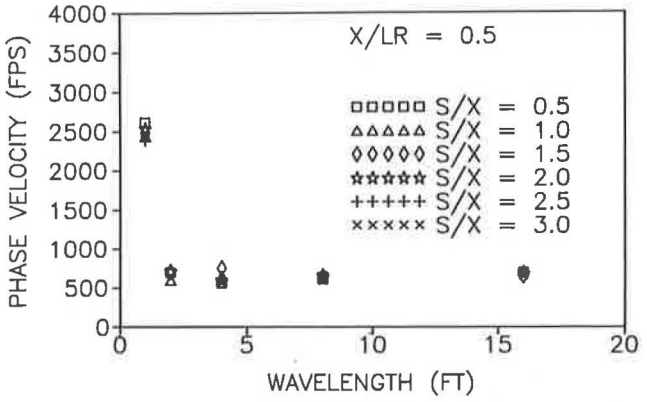

FIGURE 10 Experimental dispersion curves for $X/L_R = 0.5$ at G. G. Brown parking lot site.

Third, the measured phase velocities are practically independent of S/X for values of X/L_R of 0.5 (Figure 10) or greater, for all wavelengths. This condition suggests that body wave energy is insignificant if the wave has traveled at least one-half cycle between the two receivers. Thus, the assumption of plane Rayleigh waves can be made if wavelengths longer than $2X$ are eliminated from the data. [The work of Hiltunen (*10*) supports these observations.]

Combined Dispersion Curves

Effects of Source-to-Near-Receiver Distance (S)

The effects of S on the combined experimental dispersion curves were obtainable from the test data. The dispersion curves resulted from using an averaging algorithm for combining the data obtained for all values of X. They are also the dispersion curves that would be used in the inversion process for determining a stiffness profile. Two curves are shown for each value of X and S. The first curve, shown in Figure 11, is designated as "unfiltered," meaning that it contains data for all frequencies not eliminated from the field data because of poor phase or poor coherence. The second curve, shown in Figure 12, is designated as "filtered," meaning that the wavelength and receiver spacing filter criterion suggested in the previous section has been applied to the data. All wavelengths longer than $2X$ have been eliminated from each individual dispersion curve before processing with the averaging program.

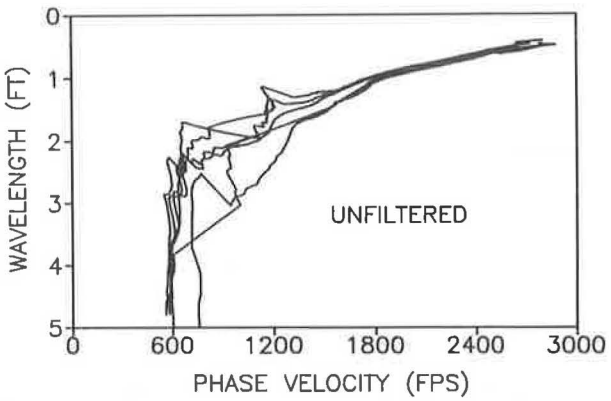

FIGURE 11 Average experimental dispersion curves (unfiltered) as a function of source-to-near-receiver distance S at SEMTA parking lot site.

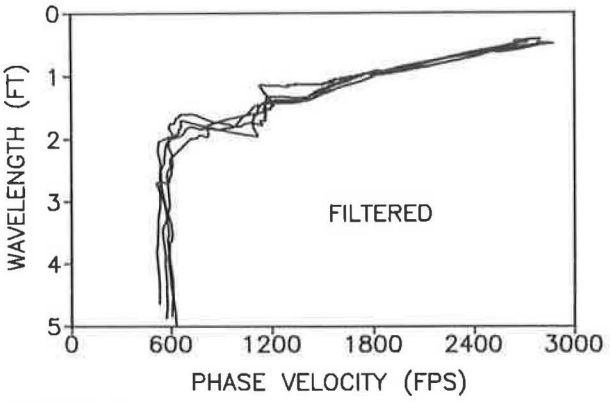

FIGURE 12 Average experimental dispersion curves (filtered) as a function of source-to-near-receiver distance S at SEMTA parking lot site.

The combined dispersion curves for the SEMTA parking lot site are shown in Figures 11 and 12. Only wavelengths from 0 to 5 ft are shown because the data for wavelengths larger than 5 ft essentially coincide, as discussed previously. [Similar plots for the G. G. Brown parking lot site have been provided by Hiltunen (*10*).]

Comparing the unfiltered with the filtered dispersion curves indicates that the recommended filter criterion substantially eliminates the dependence of the results on S. The filtered curves essentially coincide after wavelengths longer than $2X$ are removed. Because body wave energy in the signals is negligible if the waves have traveled a minimum of one-half cycle between the receivers, a new wavelength-receiver spacing filter should be implemented for SASW data analysis of pavement sites, i.e., removal of wavelengths longer than $2X$.

Effects of Source Type

This section examines the effects of source type on the combined experimental dispersion curves generated from the filtered test data, i.e., after all wavelengths longer than $2X$ are eliminated. The two dispersion curves shown on the plots in Figures 13–16 illustrate the effects of source type. First, the combined dispersion curve obtained using the optimum hammers that were identified in Table 1 is shown. By definition, the optimum hammer for a given value of X is the hammer that provides dispersion data of significant energy over the largest frequency range. The corresponding dispersion curve thus determined is the best curve for the given site. The second curve shown on the plots in Figures 13–16 is the combined dispersion curve for a constant source type, i.e., the result of combining the data obtained for all receiver spacings using the same source. The goal was to determine the minimum number of sources required to adequately define the dispersion curve for a given site.

Combined dispersion curves for both the SEMTA and G. G. Brown parking lot sites have been provided by Hiltunen (*10*). Five sources were used at the SEMTA parking lot site and

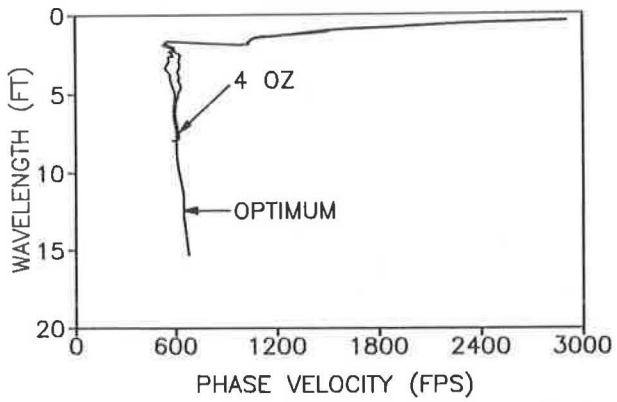

FIGURE 13 Average experimental dispersion curve for 4-oz hammer for SEMTA parking lot site (all wavelengths).

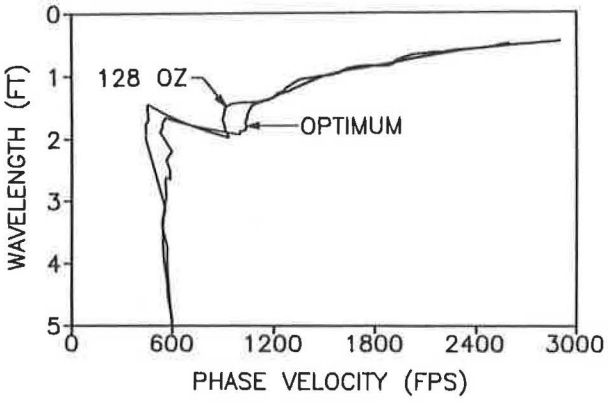

FIGURE 14 Average experimental dispersion curve for 128-oz hammer at SEMTA parking lot site (0- to 5-ft wavelengths).

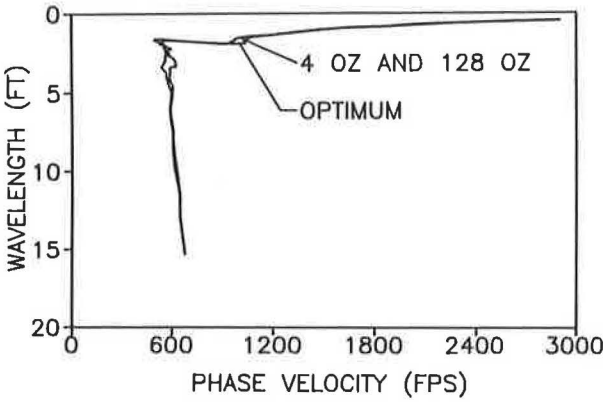

FIGURE 15 Average experimental dispersion curve for 4- and 128-oz hammers at SEMTA parking lot site (all wavelengths).

data were collected with each source at all receiver spacings (see Table 1). Only the results for the 4- and 128-oz hammers are presented here.

Figures 13 and 14 show the optimum results and the dispersion data generated from a single source type. From these plots and results reported by Hiltunen (*10*), no single source consistently duplicated the optimum results over all wavelengths. The light hammers cannot generate low enough frequencies, whereas the heavy hammers cannot generate high enough frequencies. However, in the wavelength ranges at which data exist for a constant source type, the phase velocities are nearly identical to those for the optimum results.

Because single source types fail to consistently duplicate the optimum results, Figures 15 and 16 show a comparison of the optimum results with those obtained from combining the data for the 4-oz and 8-lb hammers. These hammers were the lightest and heaviest hammers tested, respectively, and thus matched the optimum results at the high and low frequencies. The results for the overlap of the frequency ranges were also indistinguishable from the optimum results. Thus, to fully characterize the dispersion curve, only these two sources are required.

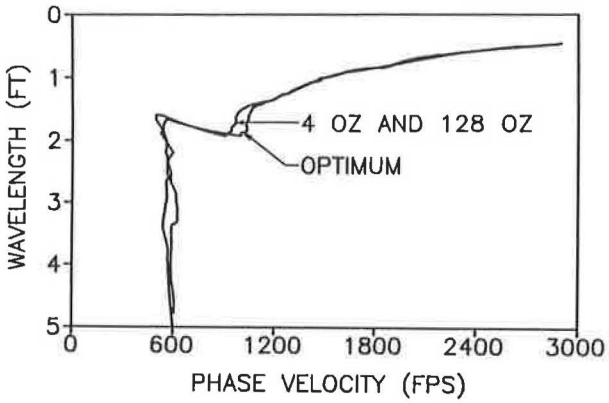

FIGURE 16 Average experimental dispersion curve for 4- and 128-oz hammers at SEMTA parking lot site (0- to 5-ft wavelengths).

SUMMARY AND CONCLUSIONS

The purpose of the research reported herein and in the research program of Hiltunen (*10*) was to further the development of the SASW method toward a practical technique for in situ investigation of pavement systems. Eventually an automated testing procedure will be developed for collecting the necessary data in the field, analogous to the deflection measurement procedures currently used in the pavement industry. The development of a multiple-transducer testing procedure is an important step toward this goal, but poses questions about (a) the source and receiver geometry, (b) location of the source, and (c) source type. A systematic experimental investigation was therefore conducted at two asphaltic concrete pavement sites on the effects of source and receiver geometry, source-to-near-receiver distance S, and source type, in the context of a multiple-transducer testing procedure. The results were independent of source and receiver geometry (*20*). The effects of S were extremely important. The ratio S/X should be ≤ 2. Phase velocity measurements were independent of S when wavelengths longer than $2X$ were filtered from the data. The effects of source type on the ranges of useful frequencies for a given receiver spacing were significant. In general, both the lower and upper cutoff frequencies decreased as the weight of the hammer increased. Single source types failed to consistently duplicate the optimum results at all frequencies. In general, the light hammers could not define the dispersion curve on the low-frequency end, and the heavy hammers could not define the dispersion curve on the high-frequency end. However, dispersion curves generated by combining the data from a 4-oz ball peen hammer and an 8-lb sledge hammer yielded the optimum results over all wavelengths.

Implications of findings [as supported by the complete research program (*10*)] for a multiple-transducer testing procedure are as follows:

- CRMP geometry would not be appropriate for a multiple-transducer testing procedure with a fixed source location because such an array could not meet the requirement that $S/X \leq 2$.
- The CS geometry with $S/X = 1$ is recommended for a multiple-transducer array.

• Use of two impact sources is a means of collecting dispersion curve data for multiple-transducer testing procedures.

ACKNOWLEDGMENT

The research described herein was supported by the Geotechnical Laboratory of the U.S. Army Engineer Waterways Experiment Station, Vicksburg, Mississippi. The authors gratefully acknowledge this support.

REFERENCES

1. D. R. Alexander, S. D. Kohn, and W. P. Grogan. Nondestructive Testing Techniques and Evaluation Procedures for Airfield Pavements. In *Nondestructive Testing of Pavements and Backcalculation of Moduli*, STP 1026, A. J. Bush III and G. Y. Baladi (eds.), ASTM, Philadelphia, Pa., 1989, pp. 502–524.
2. S. W. Lee, J. P. Mahoney, and N. C. Jackson. Verification of Backcalculation of Pavement Moduli. In *Transportation Research Record 1196*, TRB, National Research Council, Washington, D.C., 1988, pp. 85–95.
3. T. Rwebangira, R. G. Hicks, and M. Truebe. Sensitivity Analysis of Selected Backcalculation Procedures. In *Transportation Research Record 1117*, TRB, National Research Council, Washington, D.C., 1987.
4. R. L. Lytton. Backcalculation of Pavement Layer Properties. In *Nondestructive Testing of Pavements and Backcalculation of Moduli*, STP 1026, A. J. Bush III and G. Y. Baladi (eds.), ASTM, Philadelphia, Pa., 1989, pp. 7–38.
5. T. G. Davies and M. S. Mamlouk. Theoretical Response of Multilayer Pavement Systems to Dynamic Nondestructive Testing. In *Transportation Research Record 1022*, TRB, National Research Council, Washington, D.C., 1985, pp. 1–7.
6. M. S. Mamlouk. Use of Dynamic Analysis in Predicting Field Multilayer Pavement Moduli. In *Transportation Research Record 1043*, TRB, National Research Council, Washington, D.C., 1985, pp. 113–119.
7. M. S. Mamlouk and T. G. Davies. Elasto-Dynamic Analysis of Pavement Deflections. *Journal of Transportation Engineering*, ASCE, Vol. 110, No. TE6, Nov. 1984, pp. 536–550.
8. J. M. Roesset and K. Y. Shao. Dynamic Interpretation of Dynaflect and Falling Weight Deflectometer Tests. In *Transportation Research Record 1022*, TRB, National Research Council, Washington, D.C., 1985, pp. 7–16.
9. K. Y. Shao, J. M. Roesset, and K. H. Stokoe, II. *Dynamic Interpretation of Dynaflect and Falling Weight Deflectometer Tests on Pavement Systems*. Research Report 437-1, Center for Transportation Research, The University of Texas at Austin, Aug. 1986, 60 pp.
10. D. R. Hiltunen. *Experimental Evaluation of Variables Affecting the Testing of Pavements by the Spectral-Analysis-of-Surface-Waves Method*. Technical Report GL-88-12, U.S. Army Engineer Waterways Experiment Station, Vicksburg, Miss., Aug. 1988, 303 pp.
11. J. S. Heisey, K. H. Stokoe, II, W. R. Hudson, and A. H. Meyer. Determination of In Situ Shear Wave Velocities from Spectral Analysis of Surface Waves. Research Report No. 256-2, Center for Transportation Research, The University of Texas at Austin, Dec. 1982, 277 pp.
12. S. Nazarian. In Situ Determination of Elastic Moduli of Soil Deposits and Pavement Systems by Spectral-Analysis-of-Surface-Waves Method. Ph.D. dissertation, The University of Texas at Austin, 1984, 453 pp.
13. S. Nazarian and K. H. Stokoe, II. Nondestructive Testing of Pavements Using Surface Waves. In *Transportation Research Record 993*, TRB, National Research Council, Washington, D.C., 1984, pp. 67–79.
14. S. Nazarian and K. H. Stokoe, II. Use of Surface Waves in Pavement Evaluation. In *Transportation Research Record 1070*, TRB, National Research Council, Washington, D.C., 1986, pp. 132–144.
15. S. Nazarian and K. H. Stokoe, II. Nondestructive Evaluation of Pavements by Surface Wave Method. In *Nondestructive Testing of Pavements and Backcalculation of Moduli*, STP 1026, A. J. Bush III and G. Y. Baladi (eds.), ASTM, Philadelphia, Pa., 1989, pp. 119–137.
16. S. Nazarian, K. H. Stokoe, II, and R. C. Briggs. Nondestructively Delineating Changes in Modulus Profiles of Secondary Roads. In *Transportation Research Record 1136*, TRB, National Research Council, Washington, D.C., 1987.
17. S. Nazarian, K. H. Stokoe, II, R. C. Briggs, and R. Rogers. Determination of Pavement Layer Thicknesses and Moduli by SASW Method. In *Transportation Research Record 1196*, TRB, National Research Council, Washington, D.C., 1988.
18. S. Nazarian, K. H. Stokoe, II, and W. R. Hudson. Use of Spectral Analysis of Surface Waves Method for Determination of Moduli and Thicknesses of Pavement Systems. In *Transportation Research Record 930*, TRB, National Research Council, Washington, D.C., 1983, pp. 38–45.
19. J. C. Sheu, G. J. Rix, and K. H. Stokoe, II. Rapid Determination of Modulus and Thickness of Pavement Surface Layer. Presented at 67th Annual Meeting of the Transportation Research Board, Washington, D.C., Jan. 1988.
20. D. R. Hiltunen and R. D. Woods. Influence of Source and Receiver Geometry on the Testing of Pavements by the Surface Waves Method. In *Nondestructive Testing of Pavements and Backcalculation of Moduli*, STP 1026, A. J. Bush III and G. Y. Baladi, eds., ASTM, Philadelphia, Pa., 1989, pp. 138–154.
21. I. Sanchez-Salinero, J. M. Roesset, K. Y. Shao, K. H. Stokoe, II, and G. J. Rix. Analytical Evaluation of Variables Affecting Surface Wave Testing of Pavements. In *Transportation Research Record 1136*, TRB, National Research Council, Washington, D.C., 1987.

Publication of this paper sponsored by Committee on Pavement Monitoring, Evaluation, and Data Storage.